# Doping strategy to boost electromagnetic property and gigahertz tunable electromagnetic attenuation of hetero-structured Manganese dioxide

He Gaihua[1], Duan Yuping[1]*, Song Lulu[1], Zhang Xuefeng[2]

1. Key Laboratory of Solidification Control and Digital Preparation Technology (Liaoning Province), School of Materials Science and Engineering, Dalian University of Technology, Dalian 116085, P.R. China

2. School of Materials Science and Engineering, Northeastern University, Shenyang, 110819, China

Table S1 Atom percent of nickel

| Filler | Atom percent of nickel (atom%) | Reference |
|---|---|---|
| Nickeldoped MnOx/$TiO_2$ | 0.80 | [15] |
| Al-Ni-$MnO_2$ | 0.01 | [16] |
| Ni-$MnO_2$ | 0.139 | [19] |
| Nickel doped walnut-like $MnO_2$ | 3.1 | [20] |
| Nickel doped $\varepsilon$-$MnO_2$ | 15 | This work |

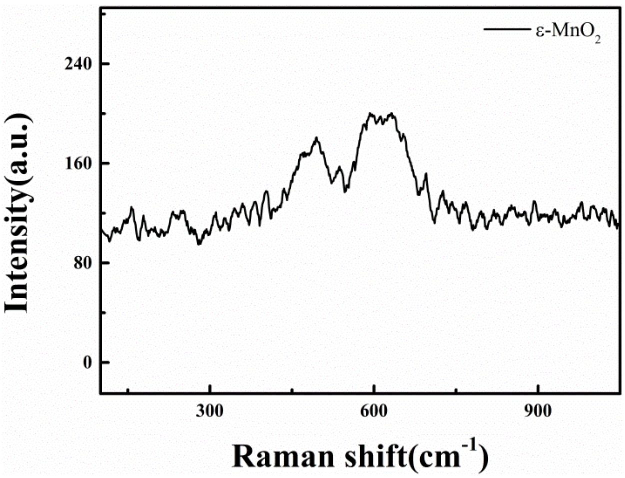


Figure S1 Raman spectra of the walnut-like nickel-doped $\varepsilon$-$MnO_2$

*Corresponding author Tel: +86 411 84708446; fax: +86 411 84708446
E-mail address: duanyp@dlut.edu.cn;

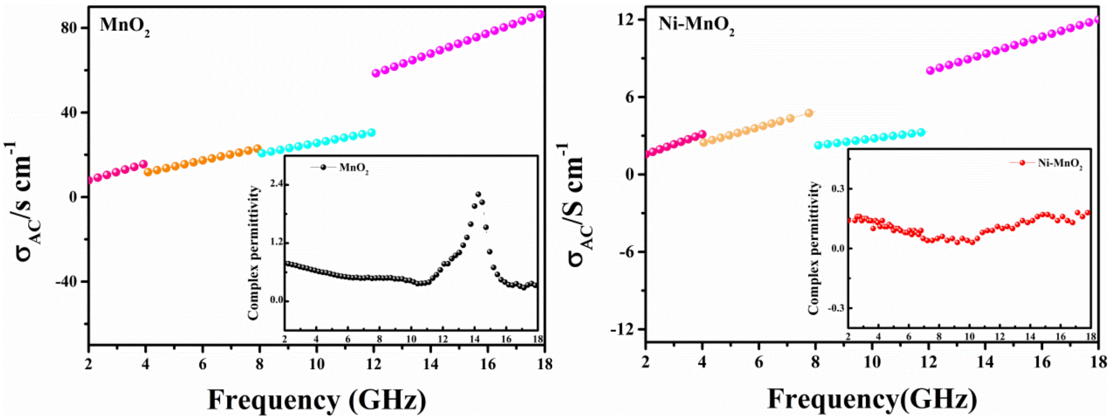


Figure S2 (a-b) Calculated electrical conductivity by the average value of ε″ at the different electromagnetic wave region of commercial $MnO_2$ and Ni-$MnO_2$

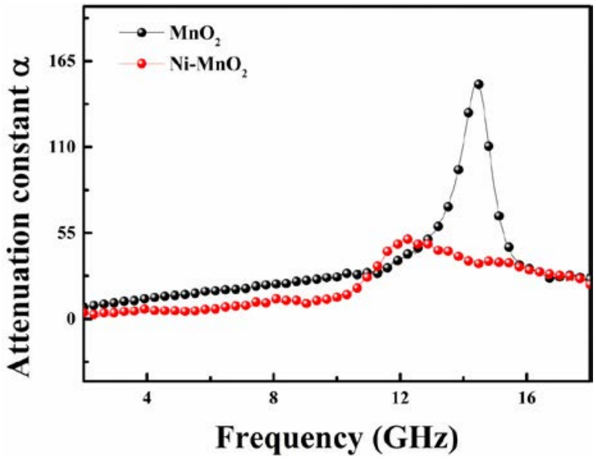


Figure S3 Attenuation constant α of commercial $MnO_2$ and Ni-$MnO_2$ versus frequency

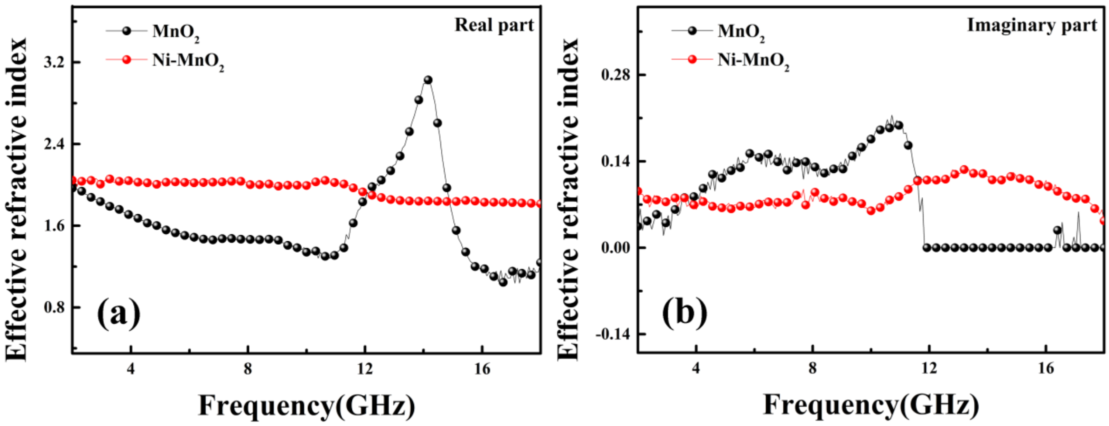


Figure S4 Real part and imaginary part of the effective refractive index of of commercial $MnO_2$ and Ni-$MnO_2$ versus frequency. The variation tendency of real part and imaginary part of the effective refractive index are very similar to imaginary part of the relatively complex permittivity and complex permeability, respectively

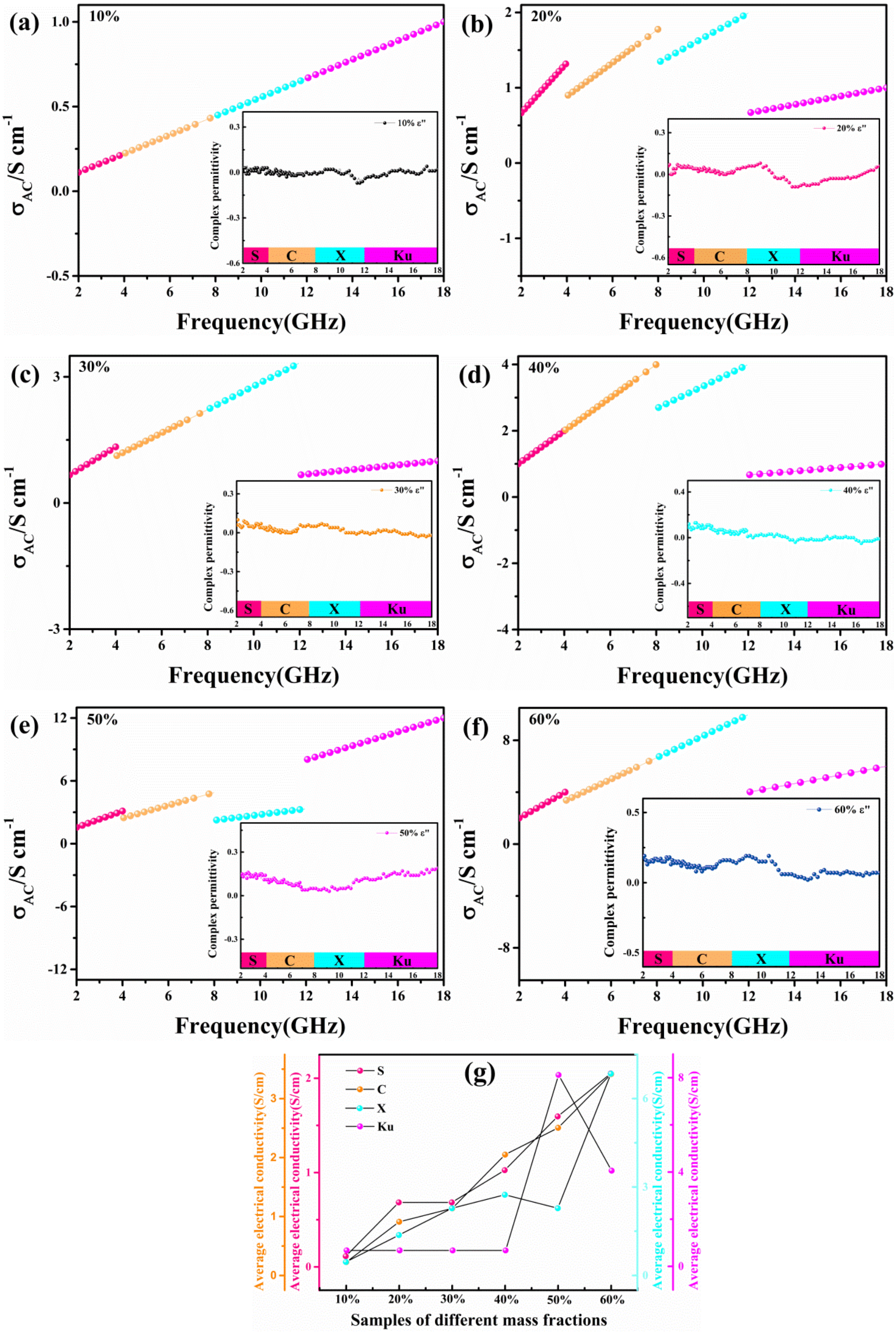

Figure S5 (a-f) the calculated electrical conductivity by the average value of ε″ at the different electromagnetic wave region of the composites with different mass fractions. The value of σ of 50% of mass fraction is relative larger, which represents energy loss refer to the orientation and polarization of dipoles. (g) line graph of the average electrical conductivity at the particular band.

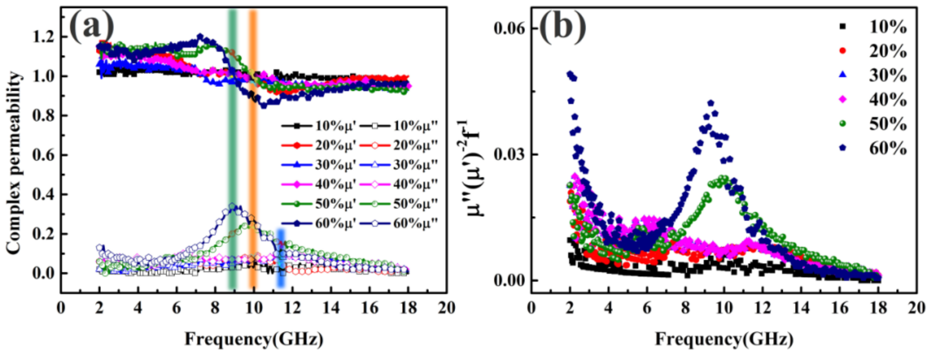


Figure S6 Electromagnetic parameters of $MnO_2$-paraffin wax composites versus frequency (a) The real part and imaginary part of the relatively complex permeability. (b) Frequency dependence of $\mu''(\mu')^{-2} f^{-1}$ of the composites with different mass fractions. The relatively complex permeability displays significant change with 50 and 60% mass fraction of walnut-like $MnO_2$ in paraffin. The value of $\mu''(\mu')^{-2} f^{-1}$ is not constant with suppressed eddy effect

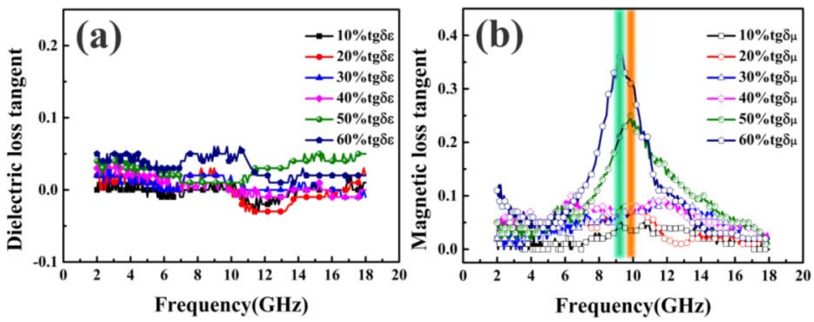


Figure S7 Dielectric loss tangent and magnetic loss tangent of the composites with different mass fractions. The $\tan\delta_{\varepsilon}$ and $\tan\delta_{\mu}$ with 50 and 60 wt% mass fraction of walnut-like $MnO_2$ in paraffin are quite similar to the frequency dependence of the $\varepsilon''$ and $\mu''$, which demonstrates that both dielectric loss and magnetic loss promote the electromagnetic wave attenuation of this sample

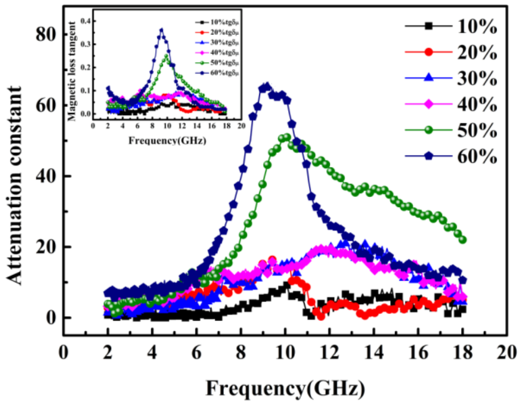


Figure S8 Attenuation constant $\alpha$ of the composites with different mass fractions. The $\alpha$ presents abruptly increase when the mass fraction of walnut-like $MnO_2$ in paraffin is up to 50%. And the variation trend is similar to imaginary part of the relatively complex permeability as well as magnetic loss tangent